

IDENTIFICATION AND LOCALIZATION OF LAYERS AND WAVE ACTIVITY IN THE ATMOSPHERE AND IONOSPHERE USING THE EIKONAL AND AMPLITUDE OF RADIO OCCULTATION SIGNALS

Alexander Pavelyev¹, Kefei Zhang², Vladimir Gubenko¹, Alexey
Pavelyev¹, Rishat Salimzjanov¹, Jens Wickert³, Yuei-An Liou⁴, C.-S. Wang²,
Yuriy Kuleshov²

¹Institute of Radio Engineering and Electronics, Russian Academy of Sciences,
Fryazino, Russia E-mail: pvlv@ms.ire.rssi.ru

²School of Mathematical and Geospatial Sciences, RMIT University, Melbourne,
Australia kefei.zhang@rmit.edu.au

³GeoForschungsZentrum Potsdam (GFZ-Potsdam), Germany [wickert@gfz-
potsdam.de](mailto:wickert@gfz-potsdam.de)

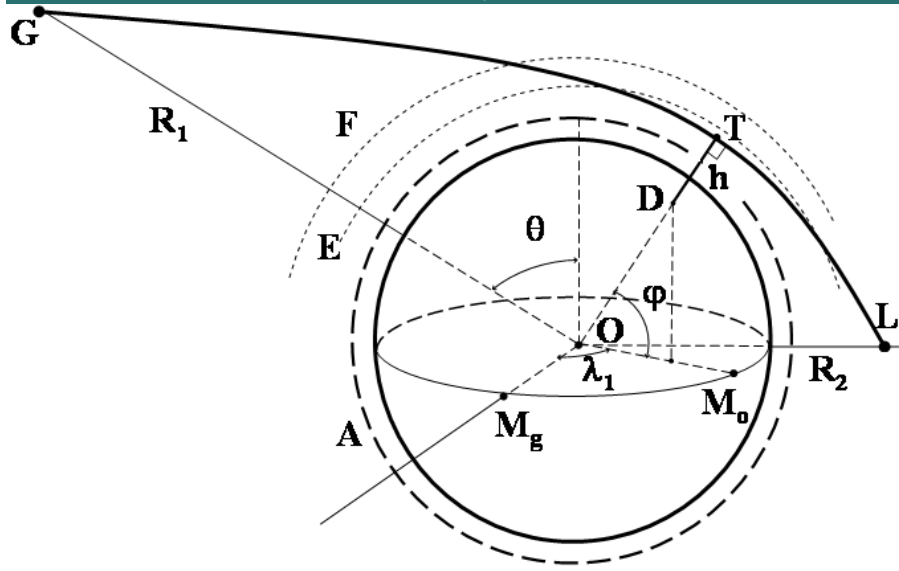
⁴Center for Space and Remote Sensing Research (CSRSR), National Central
University, Jhongli, Taiwan yueian@csrsr.ncu.edu.tw

OPAC-4 2010 September 07 Graz Austria

Outline

- (i) An analytical model is introduced for a stratified medium consisting of locally spherically symmetric sectors. Model describes different types of the ionospheric contributions to the RO signals at the altitudes 50-90 km of the RO ray perigee.
- (i) Connection between the amplitude and phase variations of the radio signals propagating in the satellite-to-satellite and satellite-to-Earth communication links. Simulation of the amplitude, bending angle and refractive attenuation of RO signal.
- (iii) Description of the eikonal acceleration technique for identification and location of layered structures in the atmosphere and ionosphere, and reflections from the Earth's surface. Possibility of the integral absorption measurements in the atmosphere.
- (iv) Possibility to separate the influence of layered structures from contributions of irregularities and turbulence in the atmosphere.

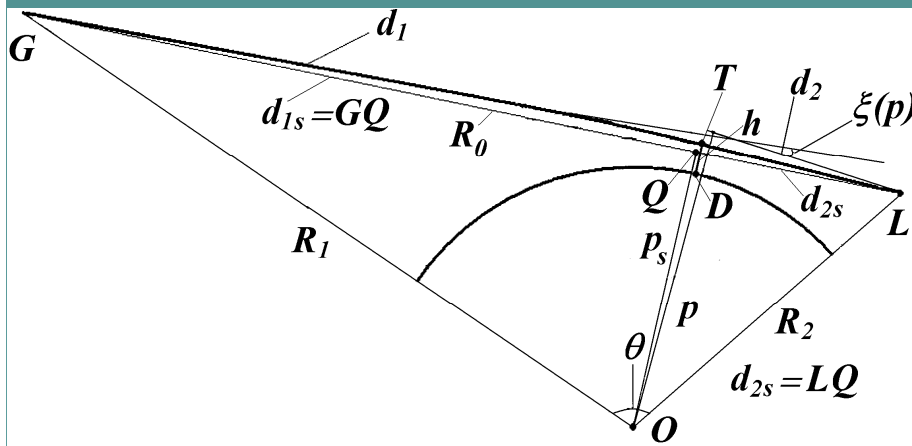
The altitude profile of the physical parameters are measured along the trajectory of tangent point T where radio waves propagate along layers. Main assumptions of RO method: (i) spherical symmetry of the atmosphere and ionosphere; (ii) there exists only one tangent point on ray GTL which coincides with radio ray perigee T. Eikonal and refractive attenuation are connected by a classical dynamic equation (Liou and Pavelyev, GRL,2006, Pavelyev et al., 2009).



$$X_L = pR_0 / [R_1R_2d_1d_2 |\partial\theta / \partial p| \sin\theta]$$

$$\Phi = \sqrt{R_1^2 - p^2} + \sqrt{R_2^2 - p^2} + p\xi(p) + \kappa(p) - R_0$$

$$\xi(p) = -d\kappa(p) / dp$$

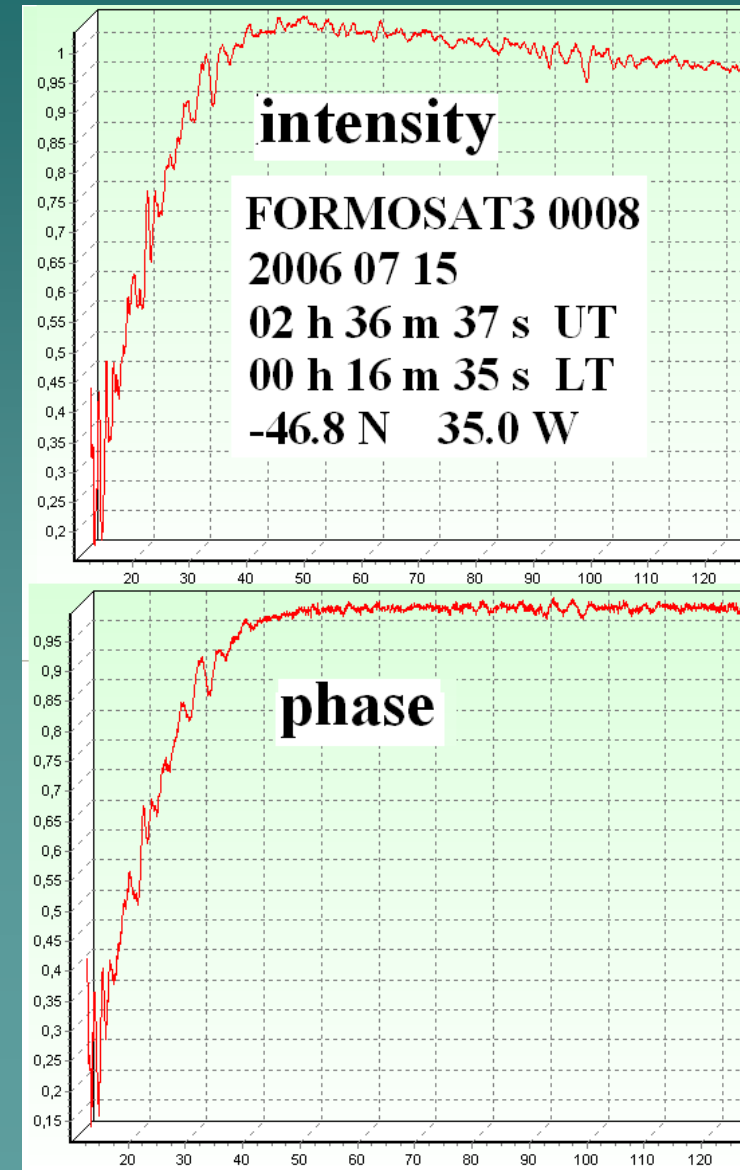
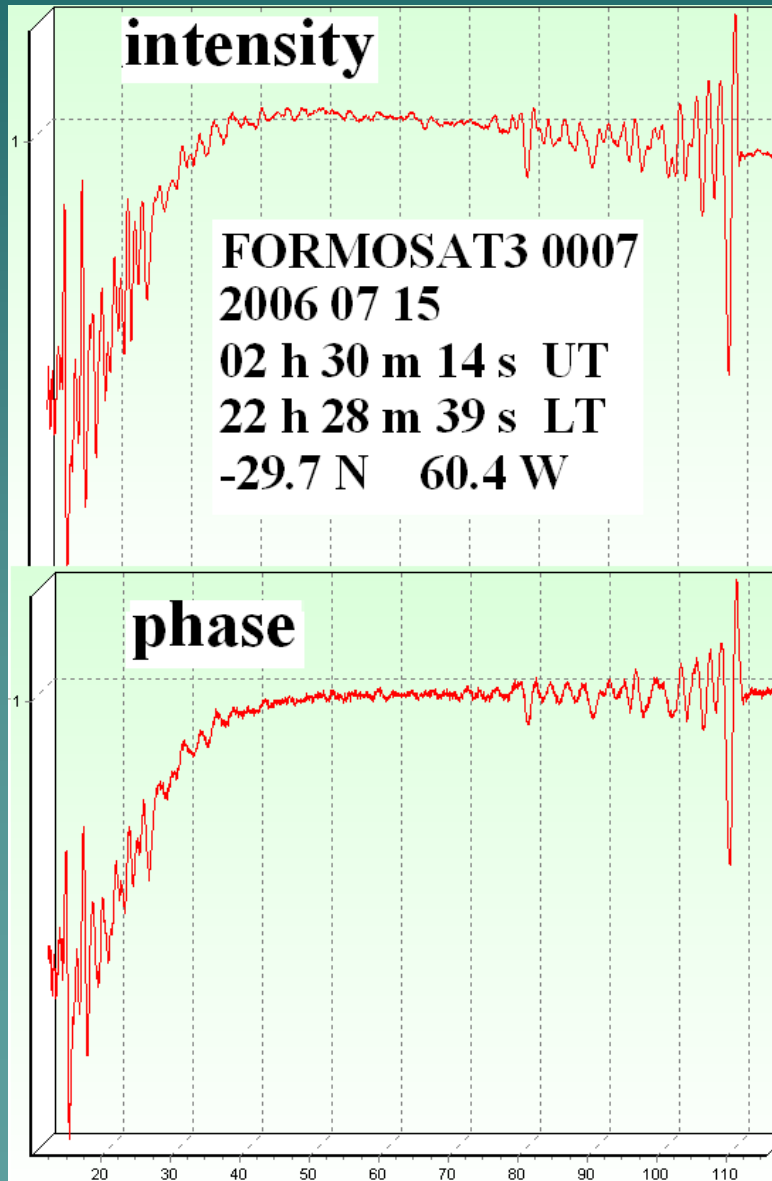


Eikonal $\Phi(p)$ and refractive attenuation $X(p)$

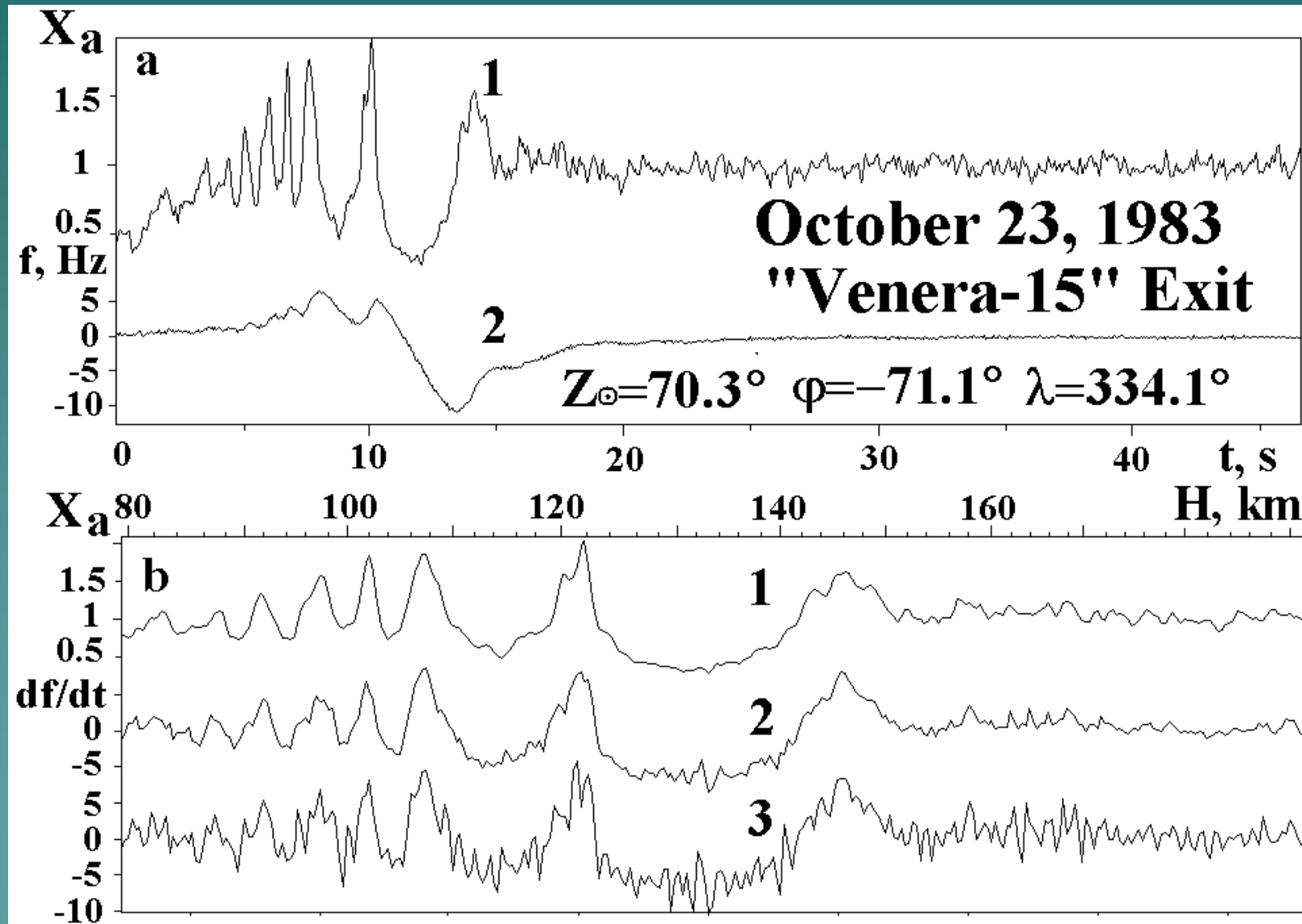
$$1 - X(p) = ma = mdF_d / dt = md^2\Phi(p) / dt^2$$

$$m = q / (dp_s / dt)^2; \quad q = (R_0 - d_2)d_2 / R_0$$

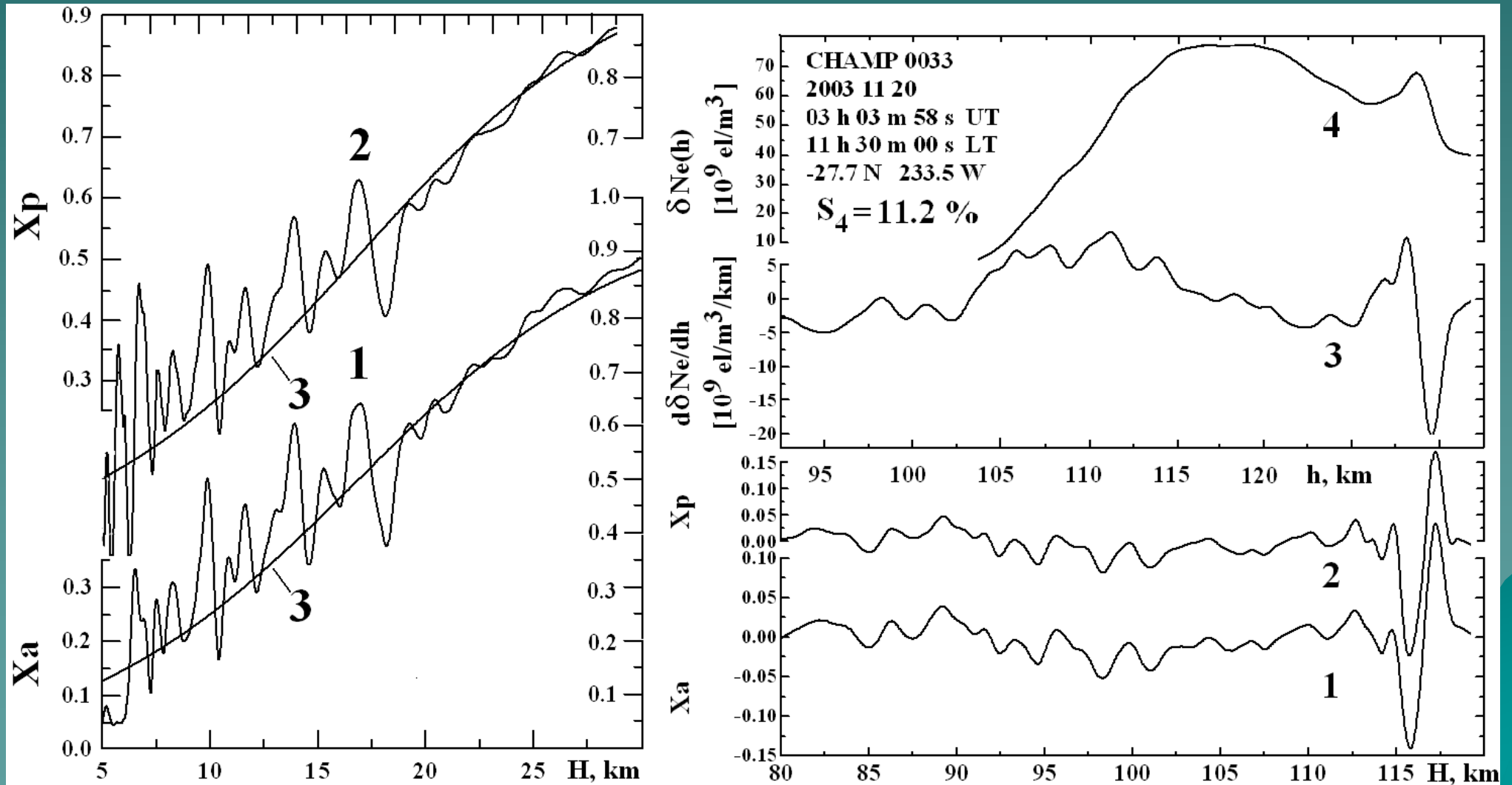
Experimental evidences of connection between the refractive attenuations X_a and X_p retrieved from the FORMOSAT-3 amplitude and phase RO data (neutral atmosphere and lower ionosphere). The antenna's amplitude diagram influence is seen in the intensity data.



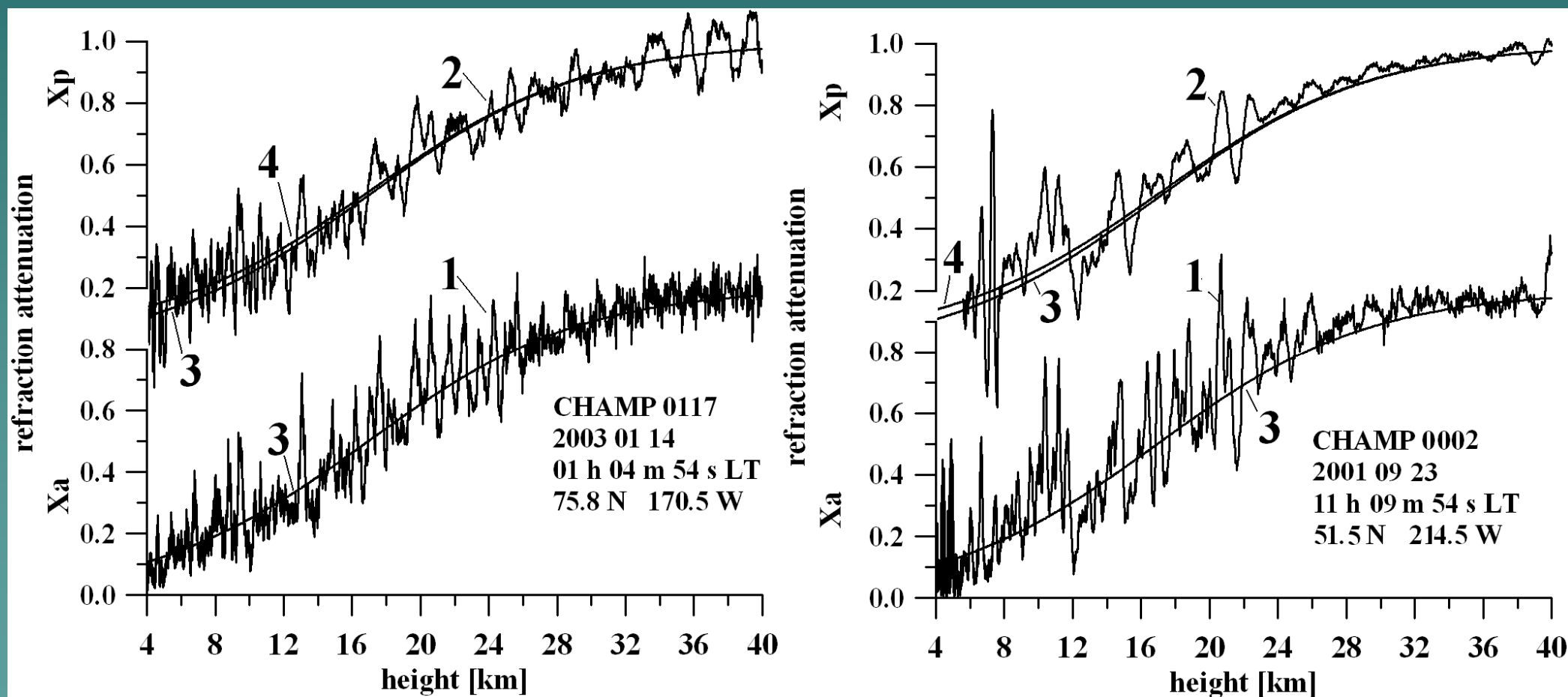
Experimental evidences of connection between the refractive attenuations X_a and X_p and derivative of the Doppler frequency on time as follows from RO data obtained during Venusian ionosphere investigation (Pavelyev et al., GRL, 2009).



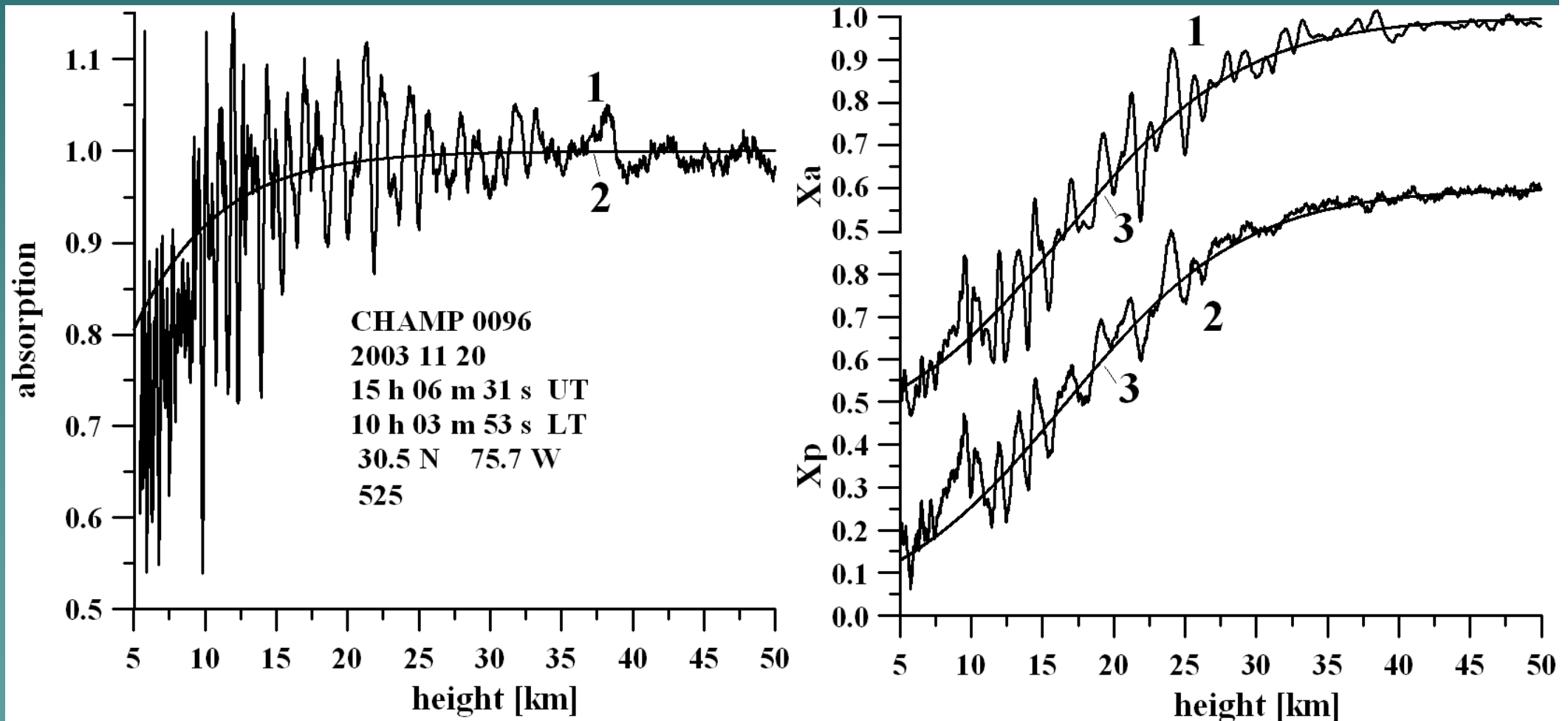
Comparison of the refractive attenuations X_p and X_a calculated from the CHAMP amplitude (curve 1) and phase data at GPS frequency F1 (curve 2). Retrieved vertical profiles of altitude profiles of electron density and its vertical gradient (curves 3 and 4, right). One may estimate the distance of the inclined ionospheric layer from the radio ray perigee and the height of the ionospheric layer by use of the eikonal/intensity technique (Pavelyev et al., GRL, 2009, GPS Solutions, 2010).



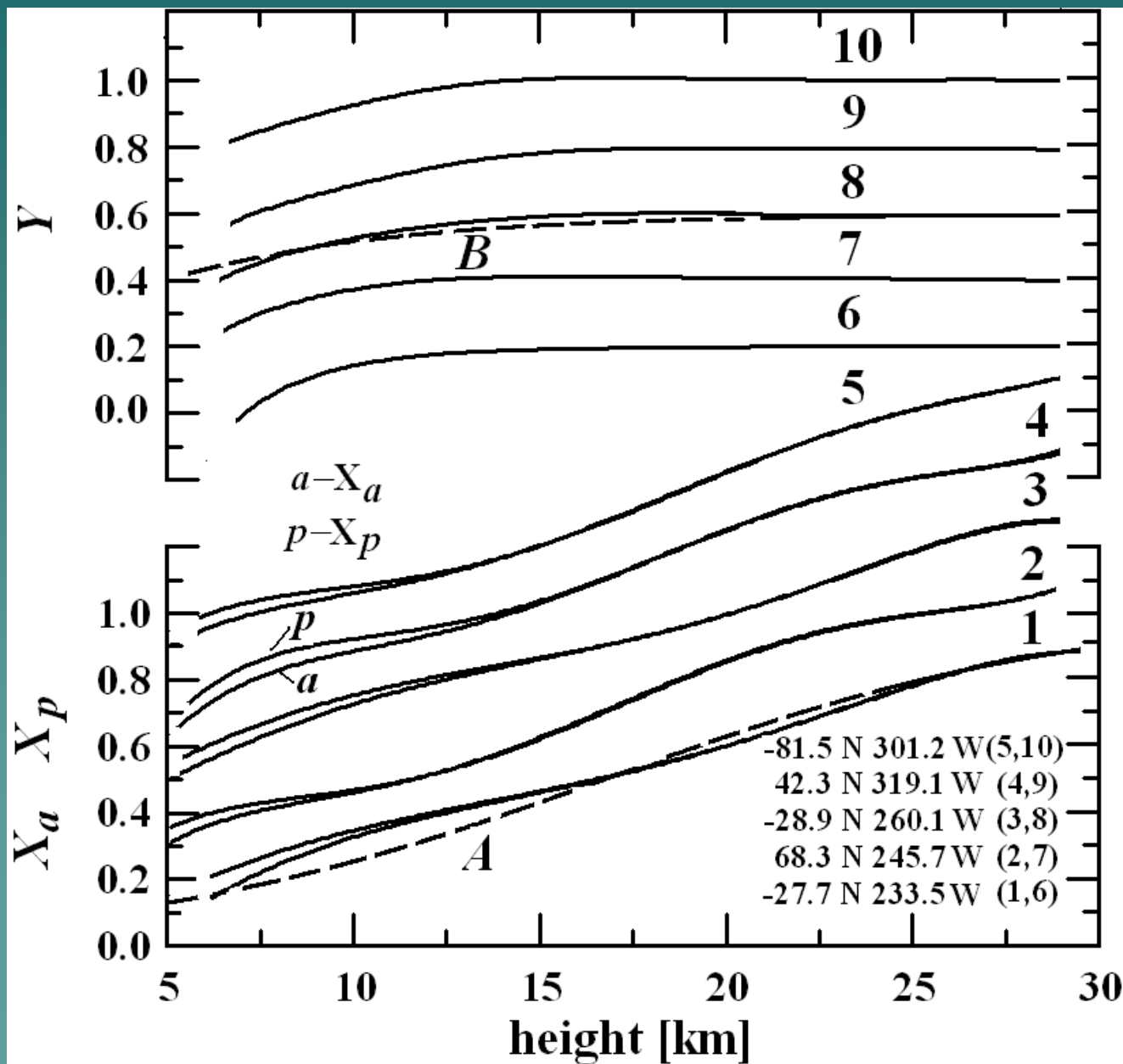
A possibility to measure absorption of radio waves by comparison of the amplitude and phase parts of the GPS radio-holograms (e.g., two events). Curves 1 and 2 describe attenuations obtained from the amplitude and phase data, respectively. Curves 3 and 4 indicate theoretical dependence of the refraction attenuation with absorption and refraction attenuation, correspondingly (Pavelyev et al., GRL, 2009).



Left: curves 1 and 2 describe experimental and theoretical altitude dependence of absorption, respectively. Right: curves 1 and 2 indicate experimental dependence of refraction attenuation calculated from amplitude and phase data. Curves 3 demonstrate theoretical dependence of the refraction attenuation and absorption.

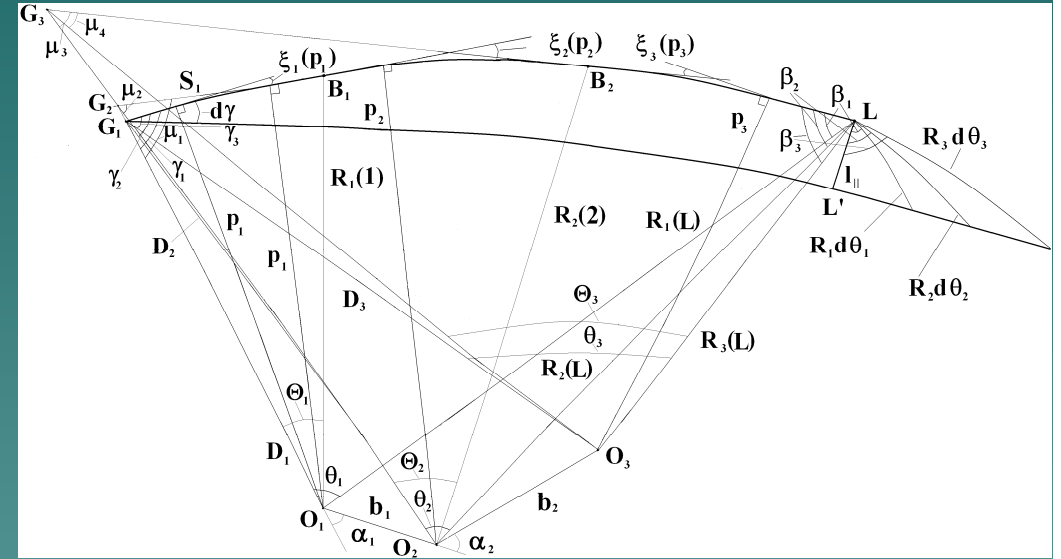
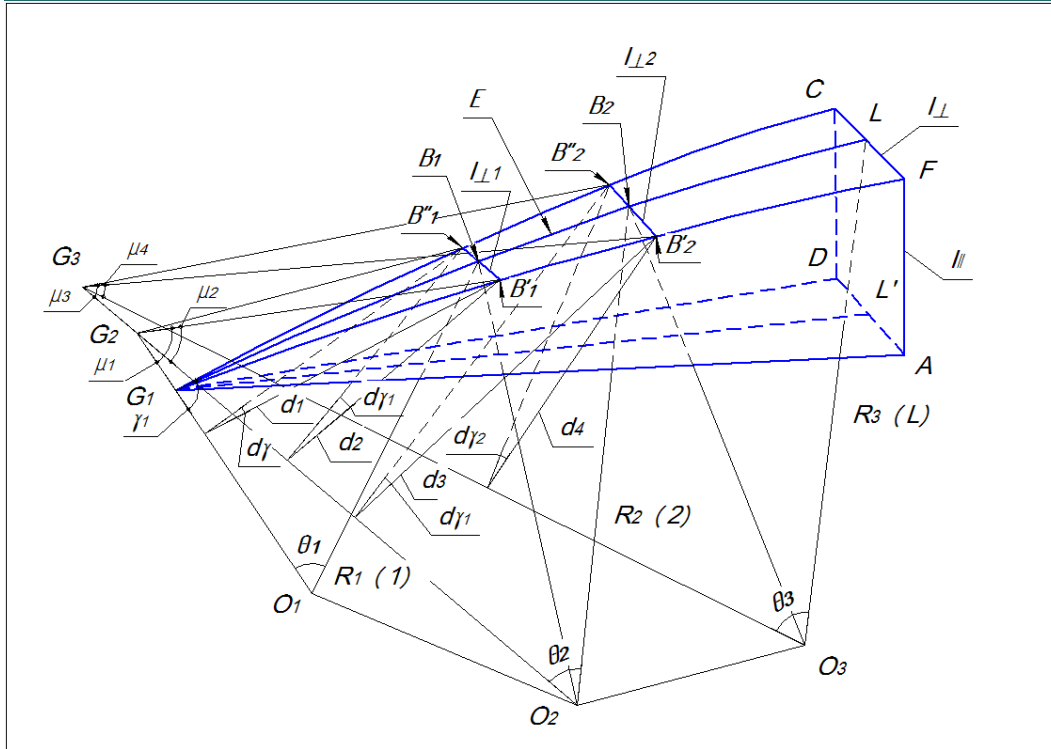


Curves 1 - 5 indicate experimental dependence of refraction attenuation calculated from amplitude and phase data. Curves 6-10 demonstrate experimental dependence of the integral absorption. Curves A,B indicated the theoretical dependence of the refraction attenuation and integral absorption (Pavelyev et al., GRL, 2009)



ANALYTICAL 3-D MODEL FOR THE PHASE PATH EXCESS AND REFRACTIVE ATTENUATION OF RO SIGNAL

Pavelyev et al., PIER 2010.
Different spherical sectors may be active during occultation.



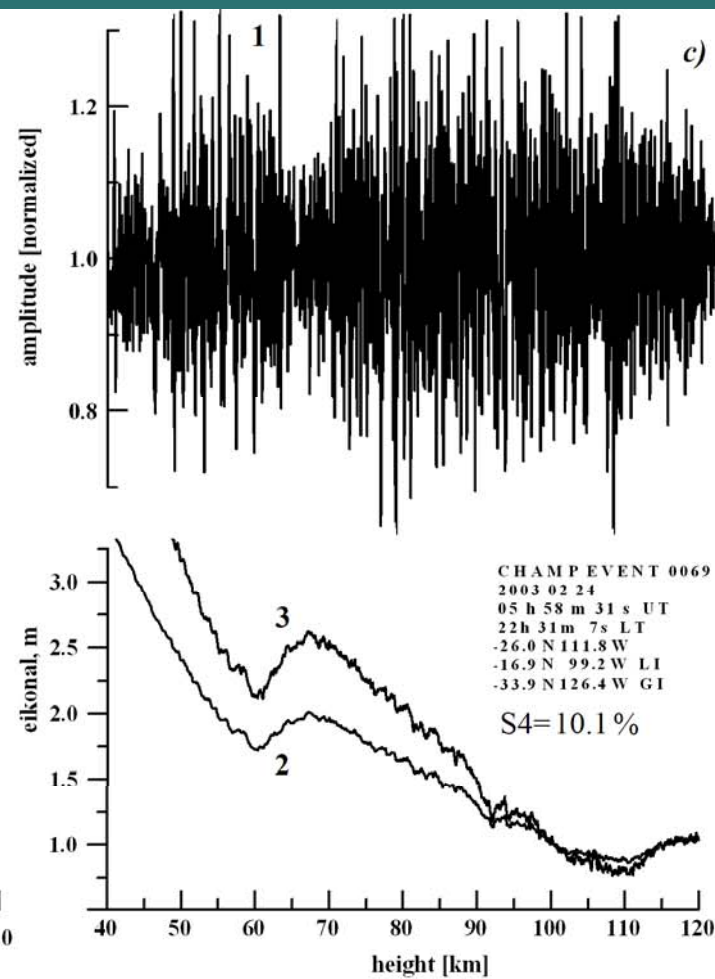
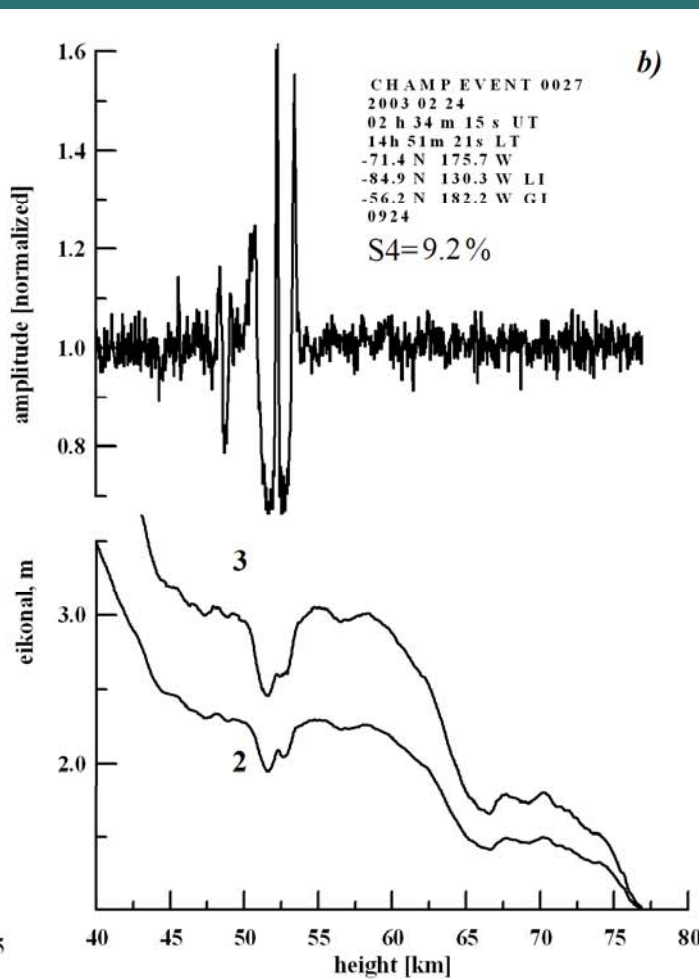
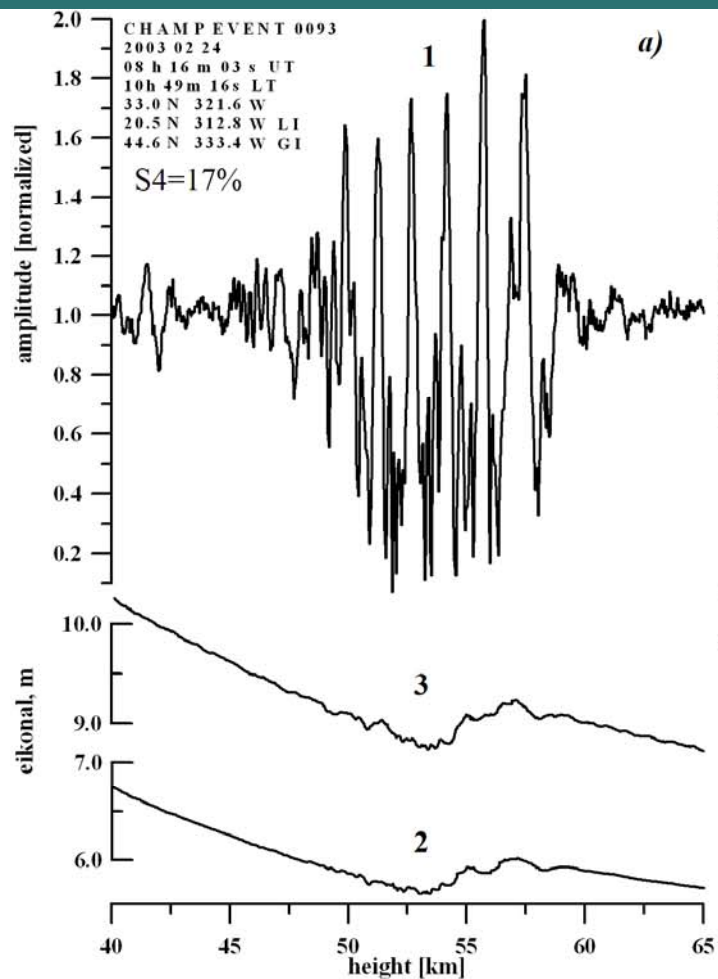
$$\Phi = \sqrt{R_1^2 - p_1^2} + \sqrt{R_N^2 - p_N^2} + \sum_{i=1}^{i=N-1} [b_i \cos(\gamma_i - \xi_i - \alpha_i) + p_i \xi_i(p_i) + \kappa_i(p_i)]$$

$$\xi_i(p_i) = -d\kappa_i(p_i) / dp_i$$

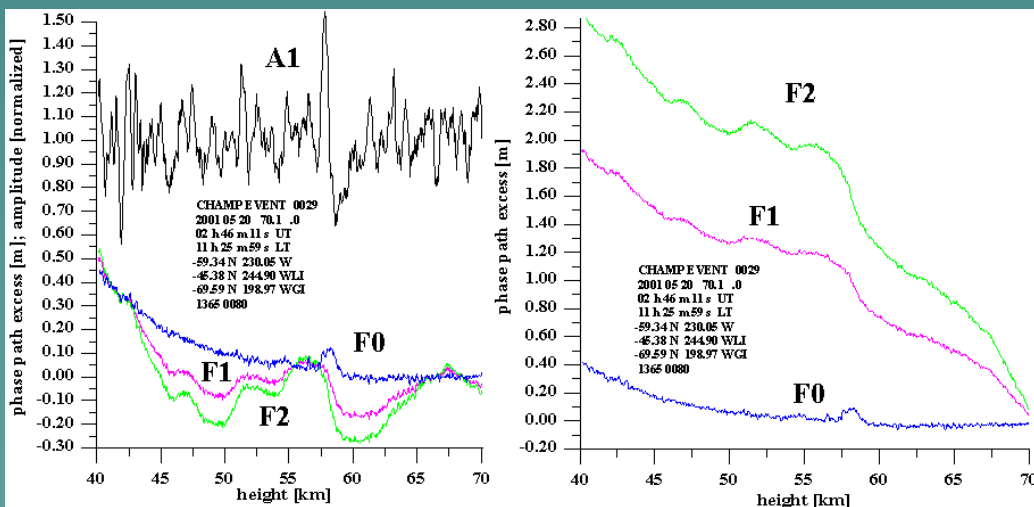
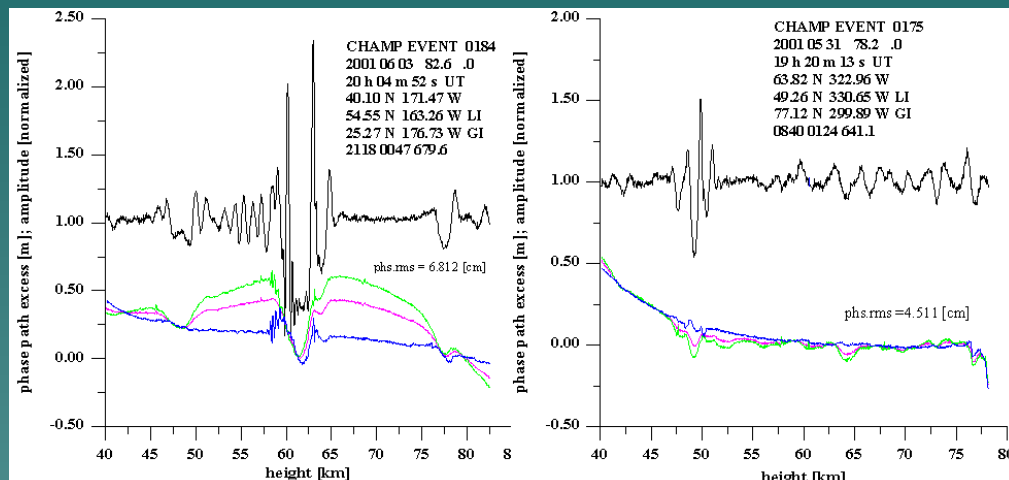
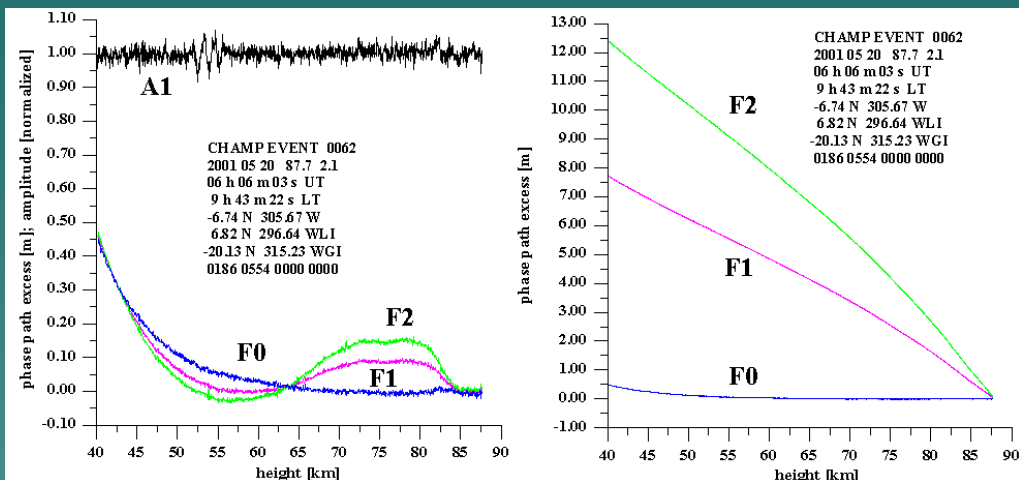
$$X_L = R_0^2 \sin \gamma_1 / \{R_i \cos \beta_i \left| \partial \theta_i / \partial \gamma_1 \right| R_N(L) \sin[\Theta_N(L)] S(1) \dots S(N)\},$$

$$i=1, \dots, N; S(i) = \sin \mu_{2i-1} / \sin \mu_{2i}, S(0) = 1$$

Types of ionospheric influence on the amplitude (A1) and eikonal (F1, F2) of radio occultation signals at frequencies 1575.42 and 1227.6 MHz in the interval 40-80 km

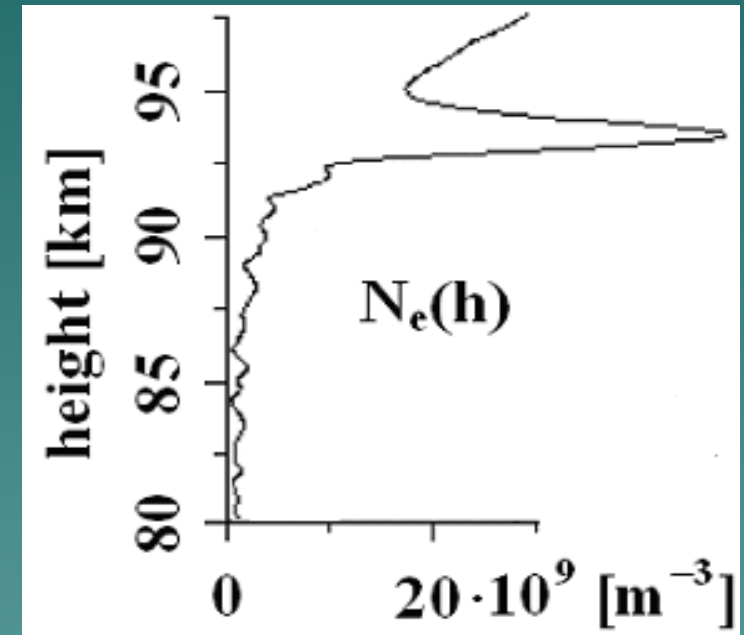
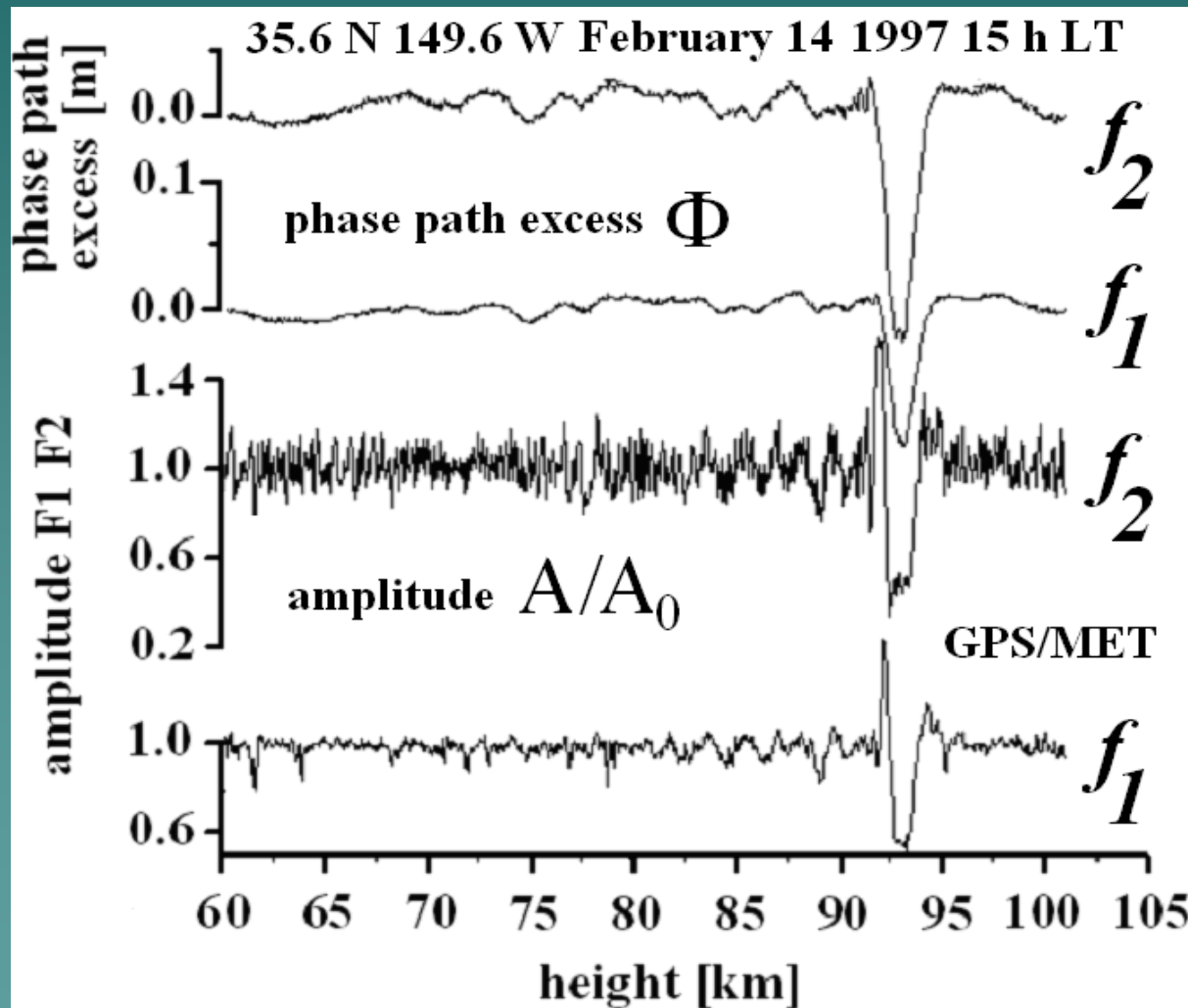


Types of ionospheric influence on the amplitude (A1) and eikonal (F1, F2) of radio occultation signals at frequencies 1575.42 and 1227.6 MHz in the interval 40-80 km

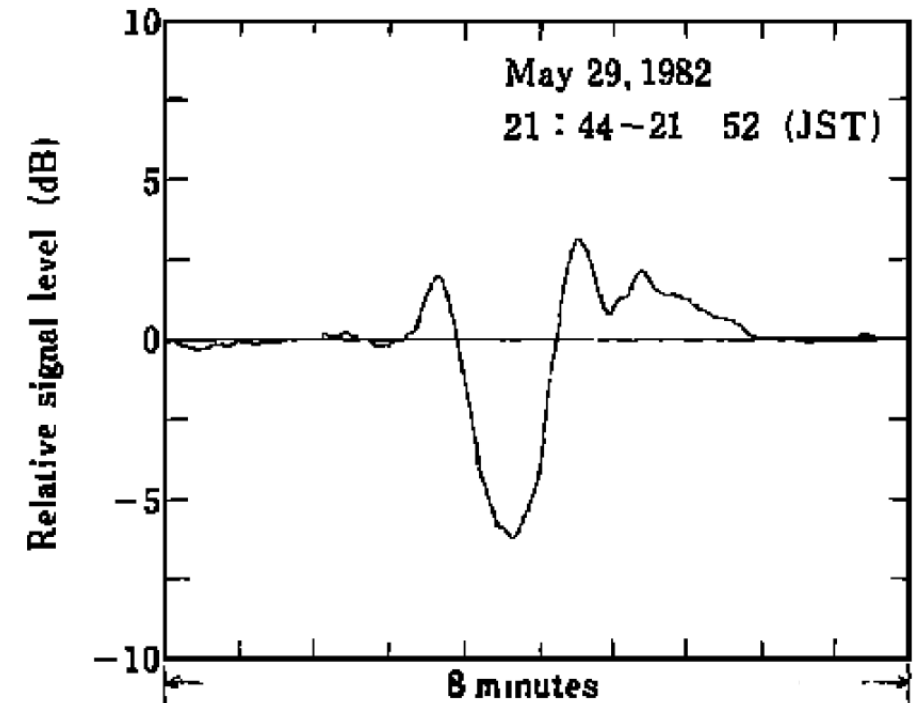
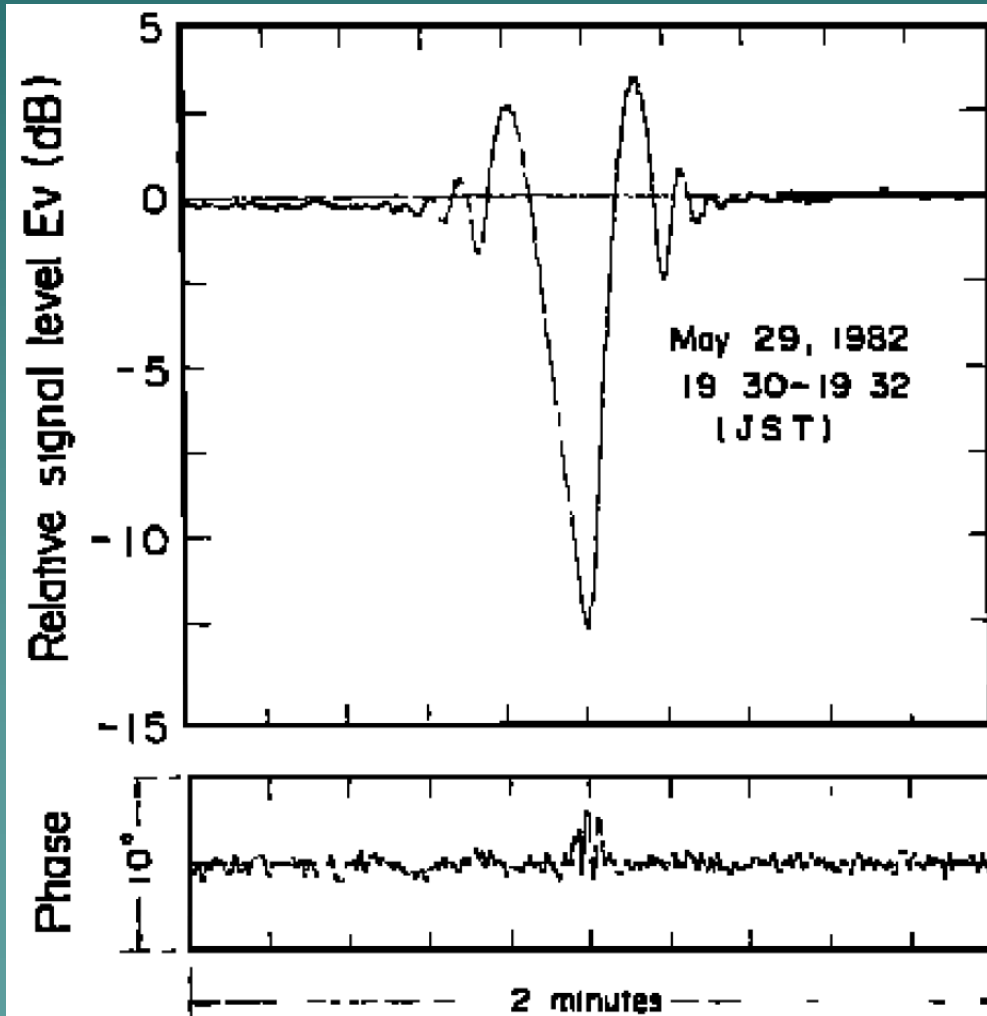


Weak ionospheric influence (top left panel)
 Strong sporadic structures influence (top right, and top bottom panel) at the altitudes of the ray perigee where expected ionospheric influence is negligible

CONNECTION BETWEEN THE PHASE PATH EXCESS AND AMPLITUDE VARIATIONS (analysis of the experimental GPS/MET data; Pavelyev et al., 2002)



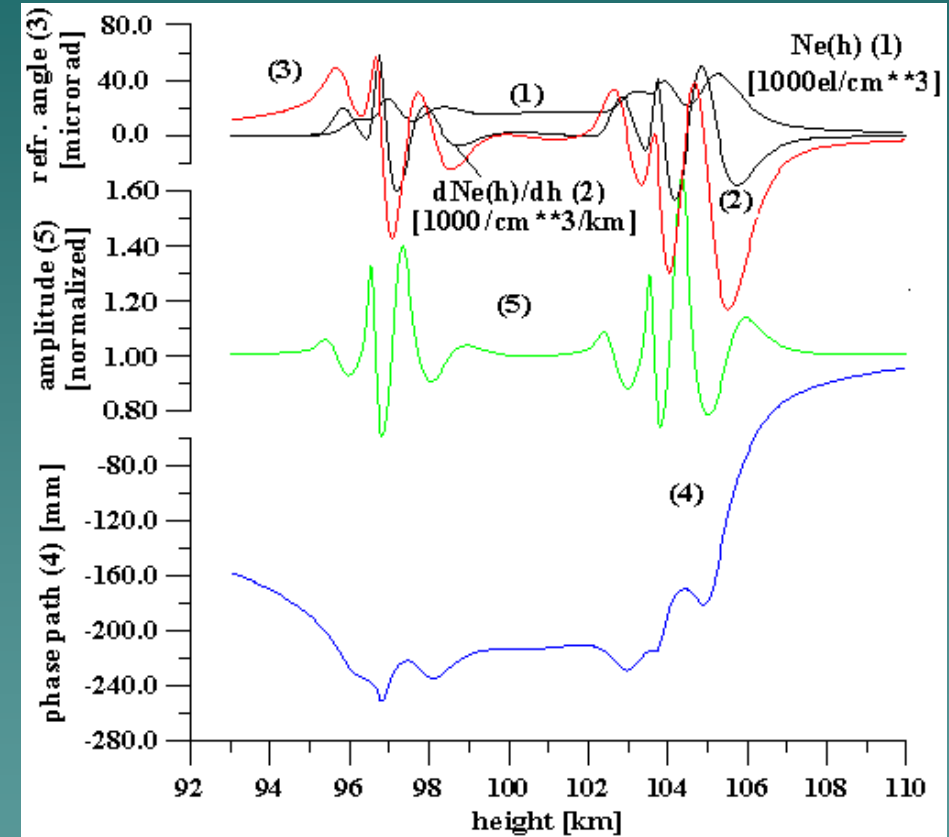
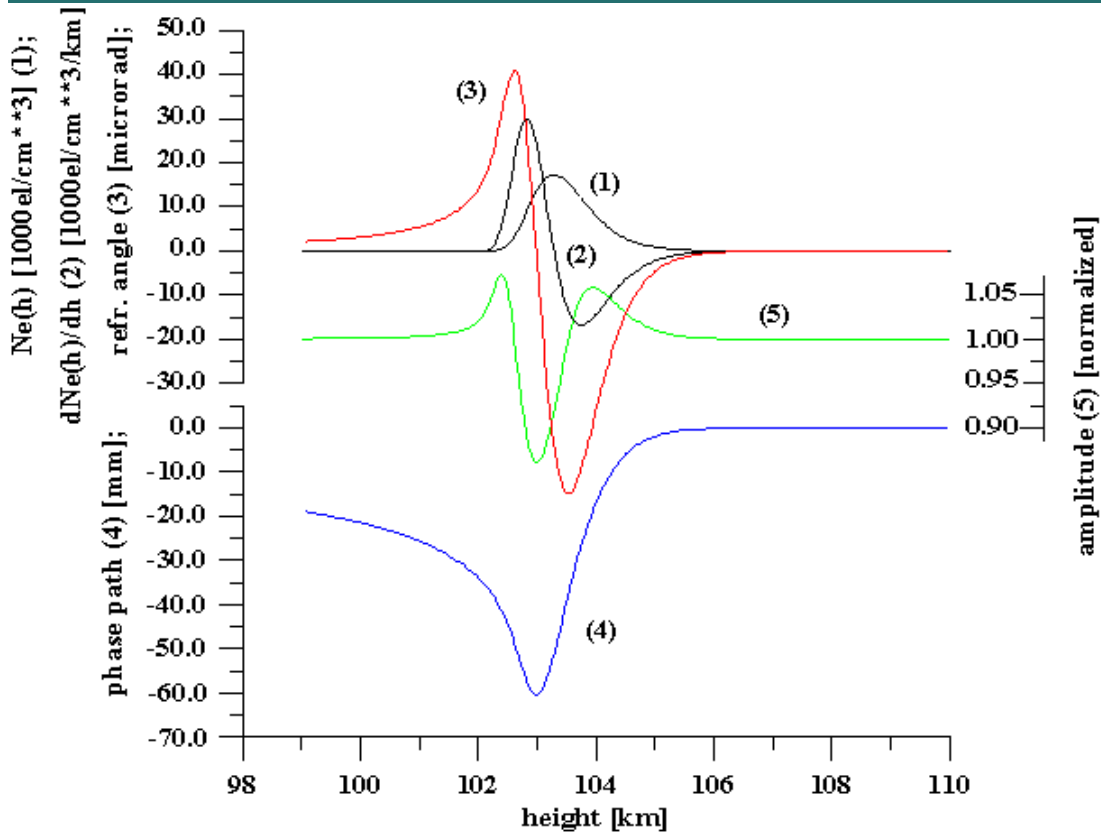
Similar amplitude variations observed in the communication link satellite – Earth (Karasawa, Radio Science, 1985)



1. Results of simulations: replies in the amplitude and phase are nearly equal to the vertical width of a layer.

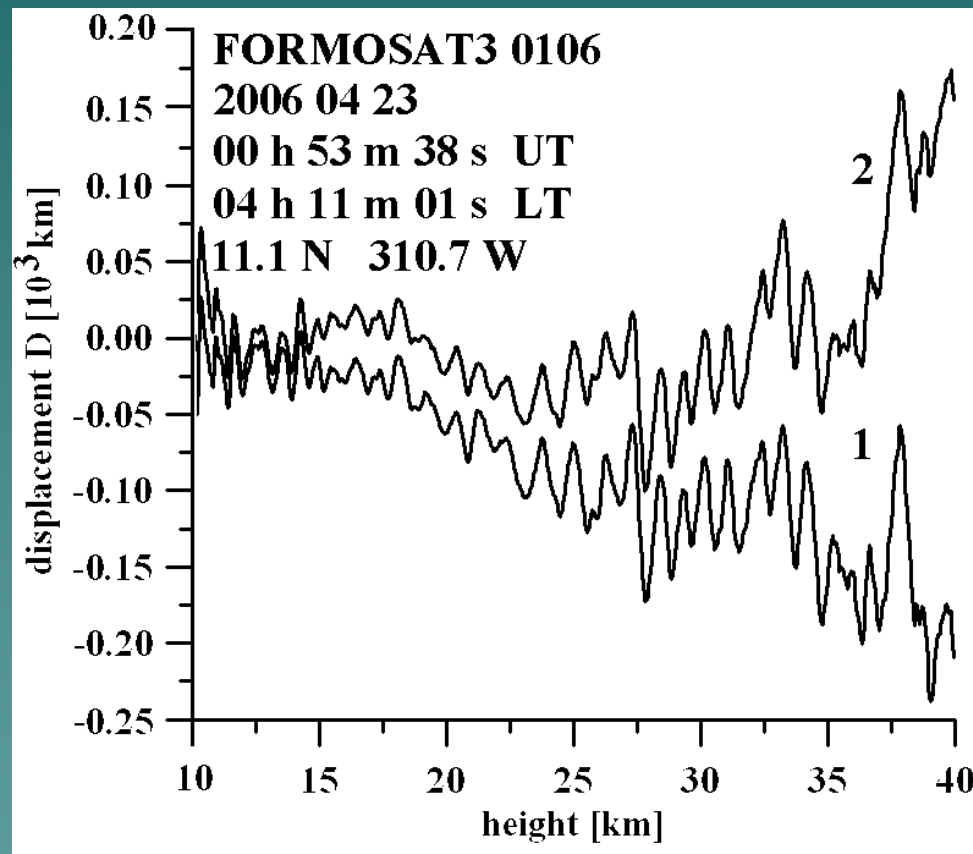
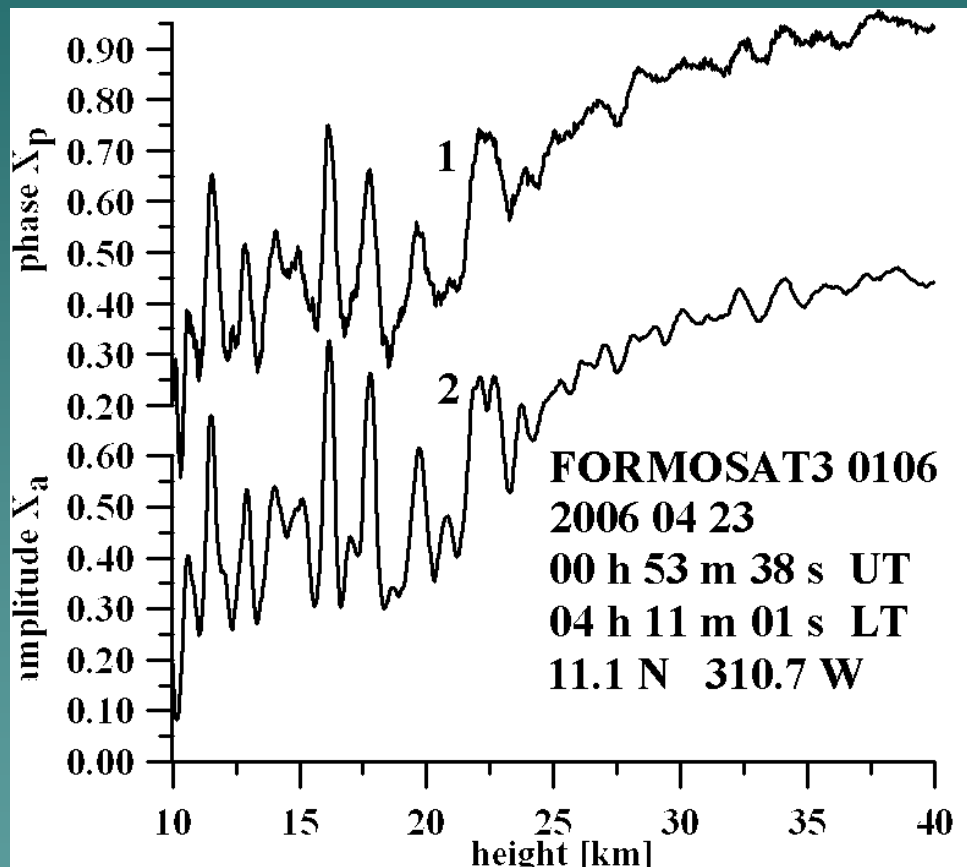
Influence of a layer on the amplitude and phase of RO signal.

Influence of seven ionospheric layers on the amplitude and eikonal variations of RO signal.

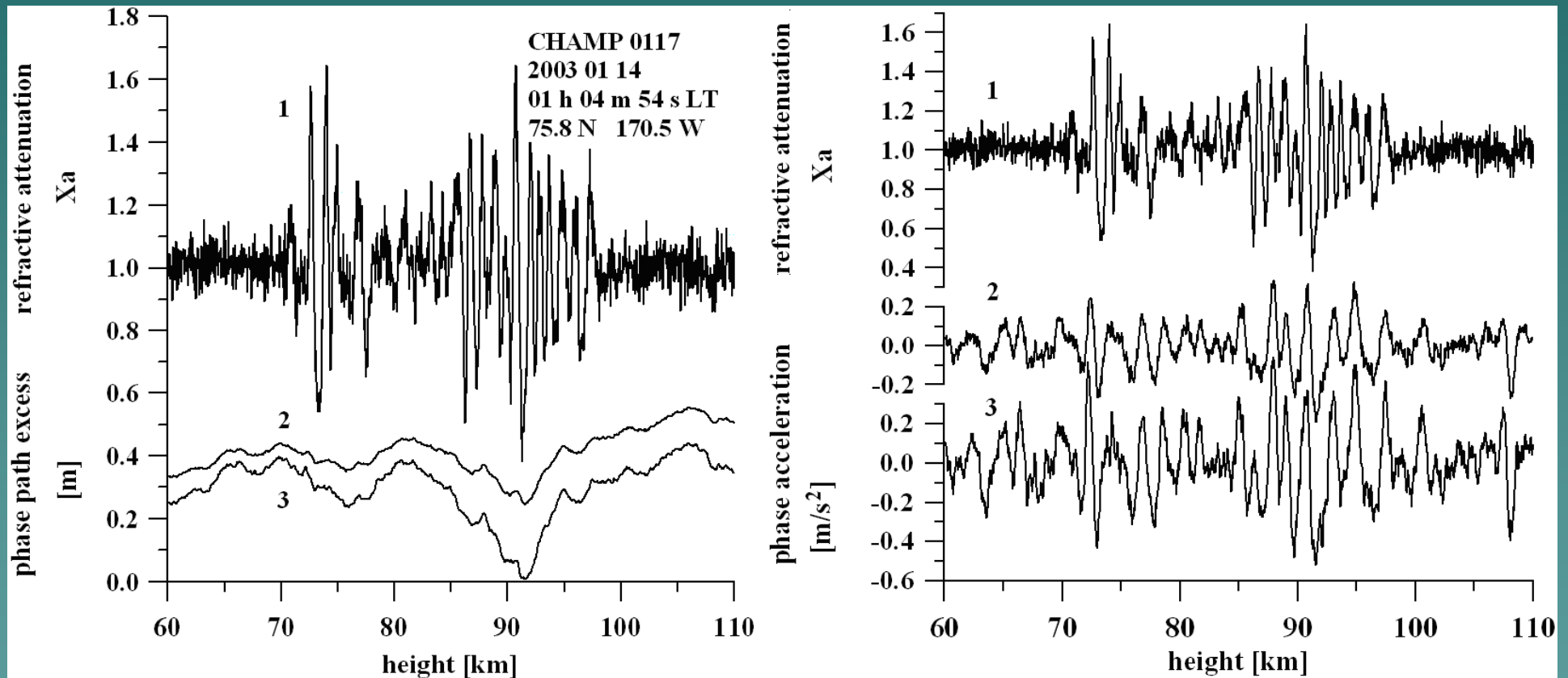


Curves 1 and 2 describe the electron density and its vertical gradient. Curve 3 corresponds to the bending angle, curve 4 and 5 are relevant to the eikonal and amplitude responses of RO signal.

Evidence of atmospheric origin of the phase and amplitude variations in RO signal. Comparison of the refraction attenuations X_p and X_a (left). Displacement D of the tangent point T from the RO ray perigee calculated from the FORMOSAT-3 phase (curve 1) and amplitude (curve 2) data (right).



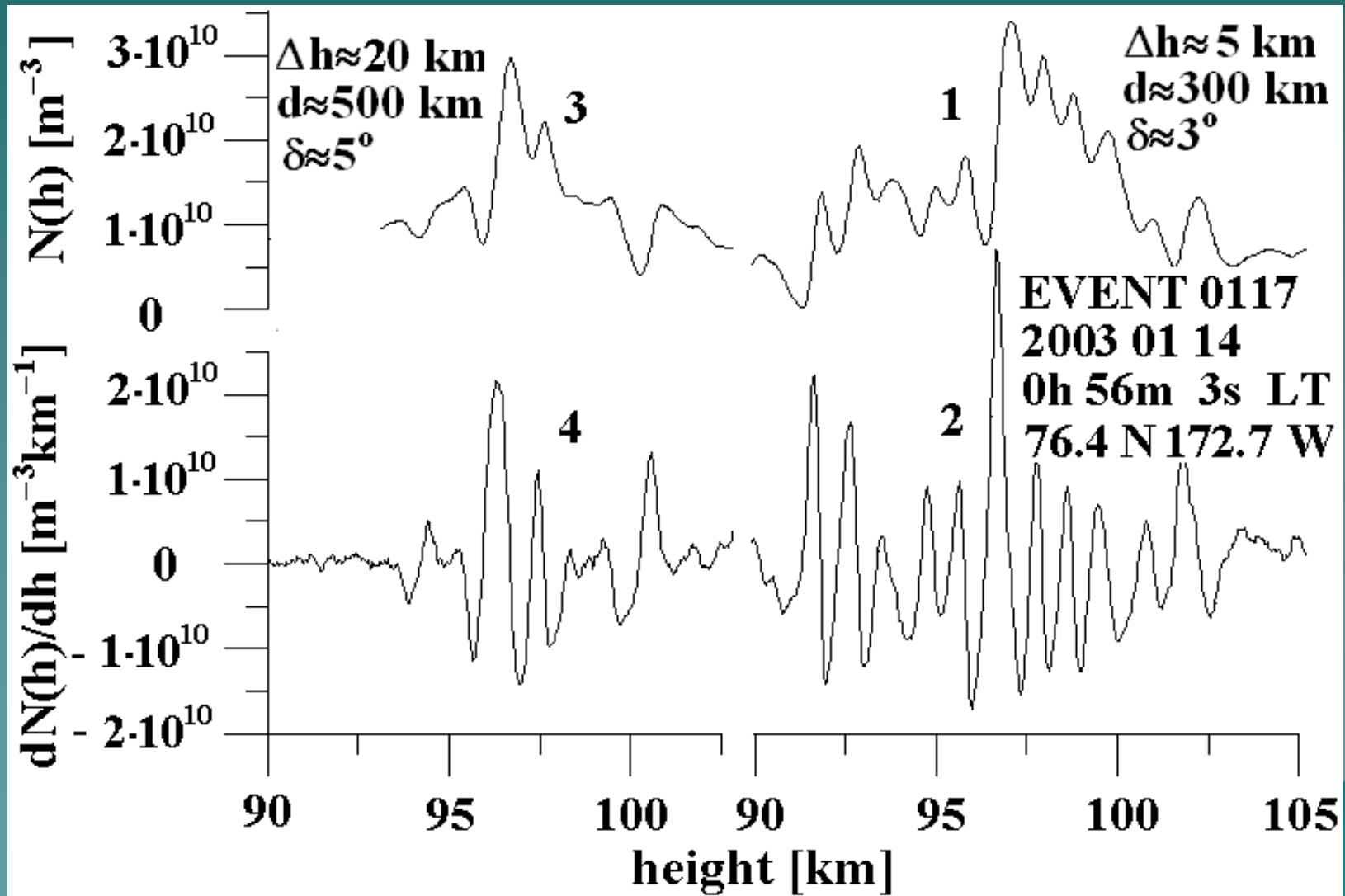
Comparison of the refractive attenuations Xa and the eikonal variations (left). Comparison of the refractive attenuation at the first GPS frequency (curve 1) and the eikonal accelerations at the frequencies F1 and F2 (curves 2 and 3) (right).



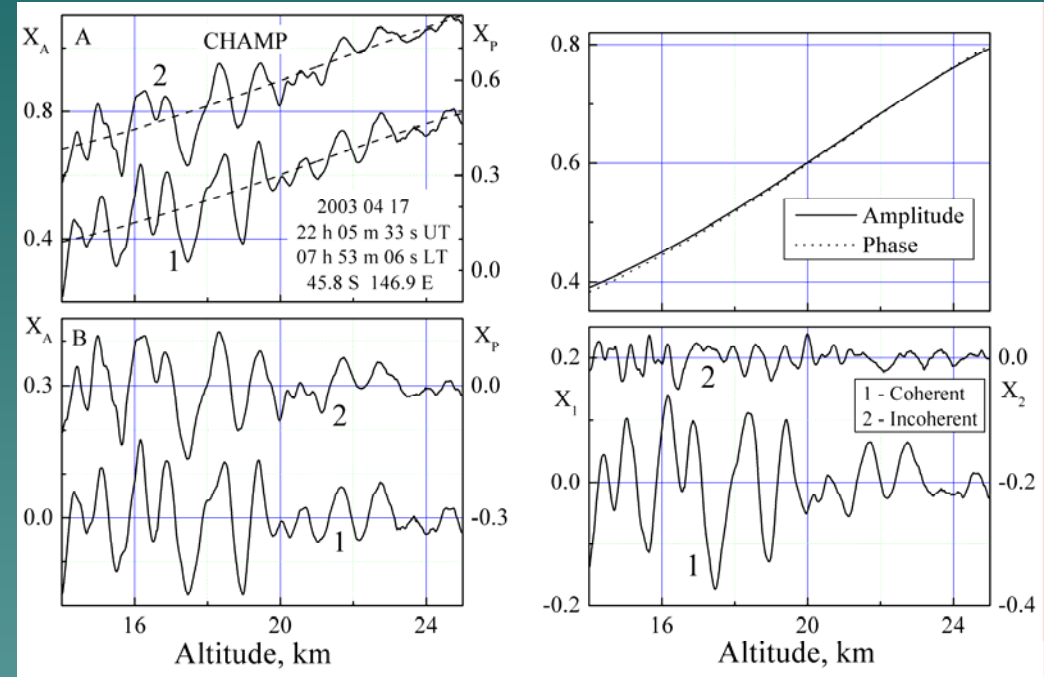
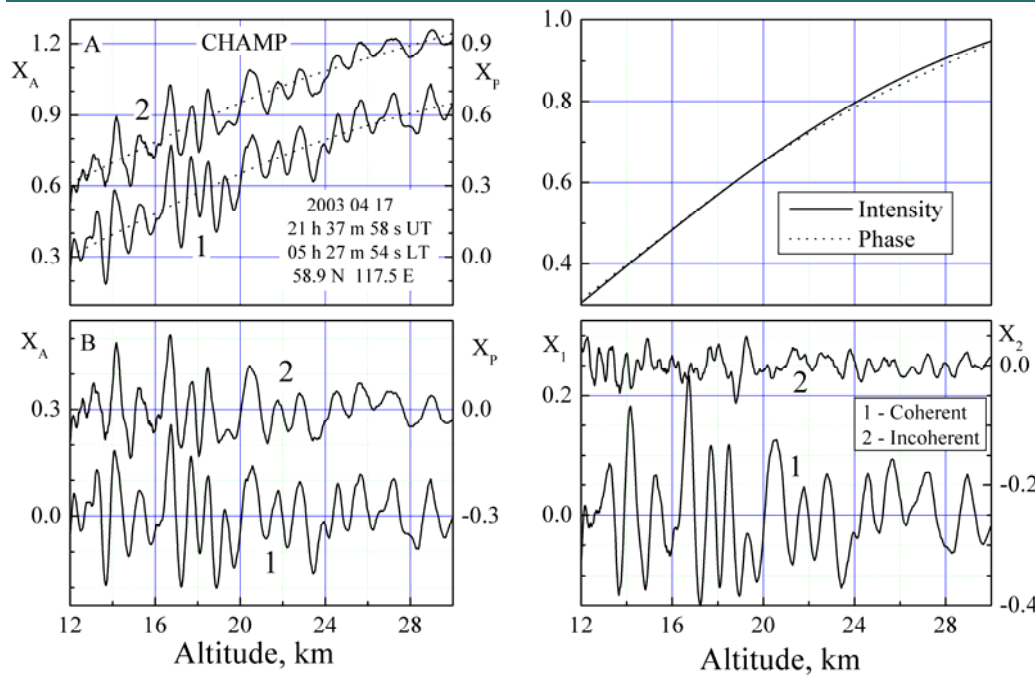
Comparison of the refractive attenuations Xa and the eikonal variations (left).
 Comparison of the refractive attenuation at the first GPS frequency (curve 1) and
 the eikonal accelerations at the frequencies F1 and F2 (curves 2 and 3) (right).

H,km	$Xp-1$	$Xa-1$	d, km	h, km	δ °	m, s ² /m
97.61	0.06429	0.07053	140.74	99.163	1.26	0.87587
97.58	0.06584	0.07291	155.00	99.461	1.38	0.88391
97.55	0.06694	0.07458	164.73	99.673	1.47	0.88940
97.52	0.06633	0.07550	198.30	100.59	1.77	0.90861
97.49	0.06610	0.07563	206.26	100.81	1.84	0.91316
97.46	0.06481	0.07478	219.46	101.22	1.96	0.92078
97.42	0.06299	0.07309	228.50	101.50	2.04	0.92599
97.39	0.06081	0.07047	226.61	101.41	2.02	0.92484
97.36	0.05814	0.06694	216.38	101.02	1.93	0.91883
97.33	0.05460	0.06265	210.95	100.81	1.88	0.91563
72.23	0.04132	0.06316	714.35	112.09	6.39	1.17436
72.19	0.04029	0.05866	626.54	102.86	5.60	1.11844
72.16	0.03934	0.05328	498.98	91.618	4.46	1.04047
72.13	0.03786	0.04721	357.26	82.105	3.19	0.95806

Vertical distribution of the electron density and its gradient in the main parts of two patches of sporadic E-layer. Curves 1 and 3 describe the electron density distribution, curve 2 and 4 relates to the vertical gradient of the electron density.



Separation of contributions from layers and irregular structures (Pavelyev and Salimzyanov, 2ordinary)



Conclusion

The eikonal acceleration has the same importance as the Doppler frequency in RO experiments. Advantages of the eikonal acceleration/intensity technique of RO data analysis are:

- (1) a possibility to separate the layered structure and turbulence contributions to RO signal
- (2) a possibility to estimate the absorption in the atmosphere by dividing the refraction attenuations found from amplitude and phase data
- (3) a possibility to locate the layered structures in the atmosphere with accuracy in the distance from the standard position of the tangent point of about ± 100 km;
- (4) a possibility to establish the ionospheric or atmospheric origin of the amplitude and phase variations of RO signal.
- (5) a possibility to estimate horizontal gradients in the lower ionosphere

Future investigations are needed to establish connections between the eikonal and amplitude variations in the general case when radio waves are propagating through locally spherically symmetrical sectors.

Thank you for your attention!

